Research paper

Performance of rubberized concrete-filled hollow steel column under monotonic and cyclic loadings

Muhammad Najmi Mohamad Ali Mastor[1], Mariyana Aida Ab Kadir[2,3], Nurizaty Zuhan[4], Kasali Adebayo Mujedu[5], Mohd Zamri Ramli[6], Ramadhansyah Putra Jaya[7], Norhazilan Md Noor[8], Mohamad Syazwan Ahmad Shah[9]

Abstract: Concrete-filled hollow steel (CFHS) has become more popular due to its advantages and benefits compared to reinforced concrete. This paper presents the experimental investigation on the performance of rubberized pozzolanic concrete-filled hollow steel column (RuPCFHS) under monotonic and cyclic lateral load in comparison to bare hollow steel column and normal concrete-filled hollow steel column (NCFHS). The test parameters included the type of concrete infill and the level of axial load. Modified rubberized pozzolanic concrete with comparable compressive strength to that of normal concrete was used. Two types of axial load conditions: no axial load and 20% axial load were considered in the testing. The test results indicate that the performance of the columns improved when concrete infill

[1]PhD Candidate, School of Civil Engineering, Universiti Teknologi Malaysia, 81310 Skudai, Johor Bahru, Johor, Malaysia, e-mail: muhammadnajmi.nst@gmail.com, ORCID: 0000-0002-8776-6900
[2]PhD., Eng., School of Civil Engineering, Universiti Teknologi Malaysia, 81310 Skudai, Johor Bahru, Johor, Malaysia, e-mail: mariyanaida@utm.my, ORCID: 0000-0002-0299-5254
[3]PhD., Eng., Institute of Noise and Vibration, Universiti Teknologi Malaysia, 81310 Skudai, Johor Bahru, Johor, Malaysia, e-mail: mariyanaida@utm.my, ORCID: 0000-0002-0299-5254
[4]PhD Candidate, School of Civil Engineering, Universiti Teknologi Malaysia, 81310 Skudai, Johor Bahru, Johor, Malaysia, e-mail: nurizatyzuda@gmail.com, ORCID: 0000-0003-3114-2960
[5]PhD Candidate, School of Civil Engineering, Universiti Teknologi Malaysia, 81310 Skudai, Johor Bahru, Johor, Malaysia, e-mail: bayomujedu@yahoo.com, ORCID: 0000-0002-1655-840X
[6]PhD., Eng., School of Civil Engineering, Universiti Teknologi Malaysia, 81310 Skudai, Johor Bahru, Johor, Malaysia, e-mail: mohdzamri@utm.my, ORCID: 0000-0002-6277-8104
[7]PhD., Eng., Faculty of Civil Engineering Technology, Universiti Malaysia Pahang, 26300 Gambang, Kuantan, Pahang, Malaysia, e-mail: ramadhansyah@ump.edu.my, ORCID: 0000-0002-5255-9856
[8]Prof., PhD., Eng., School of Civil Engineering, Universiti Teknologi Malaysia, 81310 Skudai, Johor Bahru, Johor, Malaysia, e-mail: norhazilan@utm.my, ORCID: 0000-0002-1374-0919
[9]PhD., Eng., School of Civil Engineering, Universiti Teknologi Malaysia, 81310 Skudai, Johor Bahru, Johor, Malaysia, e-mail: mohamadshazwan@utm.my, ORCID: 0000-0001-8070-4769

was introduced in the hollow steel. The application of axial loading also increased the capacity of the column specimens. RuPCFHS behaved with comparable performance with NCFHS in both monotonic and cyclic testing. RuPCFHS recorded the highest increment in the energy dissipation capability when 20% axial load was applied to the column when compared to the other specimens. The comparable performance indicated the possibility of RuPC as an infill material of CFHS and RuPCFHS as a structural component.

Keywords: concrete-filled steel tube, cyclic, lateral load, monotonic, rubberized pozzolanic concrete

1. Introduction

Concrete-filled hollow steel (CFHS) section is one of the steel-concrete composite structural elements that are available in the construction industry. The efficiency in terms of strength and stiffness of this composite element has made it an appealing option to be used in building construction. Hollow steel sections act as permanent formwork which provides a confinement effect to the concrete core, increasing the strength of the column while the concrete core delays the local buckling effect of the hollow steel section [1]. The combination of both elements comprehensively contributes to the improvement of the overall performance of the column including sufficient strength, ductility and stiffness [2]. The CFHS exhibit sufficient load-bearing capacity, ductility and energy absorption capacity. Due to its advantages over conventional reinforced concrete and steel, the CFHS has been an option for earthquake resistant structures, bridge piers, columns for supporting storage tanks, railways decks, high-rise building columns and as piles [3].

The dynamic properties possessed by CFHS are essential in earthquake-resistant structures and has attracted the attention of several authors. Elremaily and Azizinamini [4] experimentally studied the behaviour of circular concrete-filled hollow steel columns under seismic loads. The results showed that circular CFHS columns exhibited high ductility and energy-dissipation capability. The stockier columns exhibit higher energy dissipation capacity compared to slenderer columns. Han et al. [5] experimentally investigated the cyclic behaviour of concrete-filled thin-walled steel square hollow section (SHS) and rectangular hollow section (RHS) beam-columns. The specimens were tested under constant axial load and cyclically increasing flexural loading. Results showed that the ductility of columns decrease with the increase of depth-to-width ratio, concrete compressive strength and axial load level. Yuan et al. [6] had done an experiment on behaviour of partially concrete-filled steel tube (PCFST) bridge piers under bi-directional seismic excitation. The testing was carried out on circular section specimens with different concrete-filled ratios, under a series of cyclic static loading tests, and single and bi-directional hybrid (pseudodynamic) loading tests. Testing results concluded that filled-in concrete improved the seismic behaviour of steel bridge piers under single or bi-directional seismic loads compared to bare steel bridge piers, in which higher level of concrete in-fill has better performance under seismic loads. The test results suggested that conventional single-directional verification method was not able to determine the columns response under bi-directional seismic loads and should be modified.

Infill concrete plays an important role in the performance of CFHS. The properties of concrete affect the overall performance of CFHS when subjected to loadings. Following the current trend, studies have been carried out to study the performance of CFHS which utilize the usage of green concrete as infill materials. The application of crumb rubber as aggregate replacement in concrete has shown improvement in the seismic properties of the structural member. Higher damping ratio, natural frequency and peak acceleration of column utilizing crumb rubber have been reported in previous research [7, 8]. On the other hand, incorporating crumb rubber in concrete results in a decrement of axial load capacity and stiffness of the column due to the lower compressive strength of rubberized concrete.

The application of rubberized concrete as concrete infill in CFHS has been done by several authors. Duarte et al. [9] experimentally studied the cyclic behaviour of CFHS which utilized rubberized concrete as the infill material with 0%, 5% and 15% crumb rubber content. The results obtained indicate that increasing the rubber content resulted in a decrease in cyclic strength and stiffness of the columns due to the lower compressive strength and Young's Modulus of rubberized concrete. On the other hand, concrete infill with 5% crumb rubber increased the ductility of the column by about 50% that of normal concrete infill. The authors concluded that 5% was the optimum replacement percentage which showed the lowest decrease in lateral strength and the highest increase in ductility of the column. Silva et al. [10] experimentally investigated the monotonic and cyclic flexural behaviour of rubberized concrete filled hollow steel with 5% and 15% crumb rubber. The authors concluded that the type of concrete infill did not have a significant influence on the flexural behaviour of CFHS where the flexural response was mostly contributed by the steel section. However, the authors suggested that the comparison of the energy dissipation capability of the column was a more accurate measurement to study the effect of different types of concrete infill. Dong et al. [11] had studied the flexural behaviour of rubberized concrete filled hollow steel column and beam with 15% and 30% crumb rubber under eccentric loading. Higher crumb rubber content in the concrete infill resulted in improved ductility of the column, higher than that of normal concrete infill column. Also, rubberized concrete delayed the fracture of hollow steel compared to normal concrete which results in higher energy absorption and ductility of the column.

The properties of rubberized pozzolanic concrete (RuPC) using different crumb rubber and fly ash content with several water-cement (w/c) ratio was studied by Najmi et al. [12, 13]. The authors conducted an experimental investigation on the performance of rubberized pozzolanic concrete with several sets of crumb rubber and fly ash content replacing fine aggregate and cement, respectively. Results obtained from the investigation was aligned with the previous studies which indicated that the incorporation of crumb rubber in concrete decreases the overall performance of rubberized concrete compared to normal concrete (NC). Using fly ash as partial cement replacement has shown slight improvement in properties of rubberized concrete compared to rubberized concrete which only used ordinary Portland cement (OPC) as its binder. However, the improvement in properties was still lower than that of normal concrete. The optimum replacement content suggested by the authors was 5% crumb rubber replacing fine aggregate and 10% fly ash replacing OPC. In order to achieve higher rubberized pozzolanic concrete properties that

are comparable to the normal concrete, further study was carried out by modifying the rubberized pozzolanic concrete mix with the usage of a lower water-cement ratio. 0.45 was the optimum w/c ratio to be used in RuPC mix with 5% crumb rubber and 10% fly ash, which is lower than normal concrete that used 0.55 w/c ratio.

The utilization of rubberized concrete as concrete infill in CFHS exhibited a positive performance in terms of parameters important for earthquake structure such as ductility and energy dissipation. However, it can be noted that the properties of rubberized concrete infill used in the previous studies was lower than the normal concrete where crumb rubber was replaced directly with the aggregate without any modification in improving the properties of the rubberized concrete. This results in a lower axial capacity of the column, which is an important parameter required especially for column elements. Thus, in order to allow for the application of rubberized concrete as an infill material, modification in the concrete mix should be carried out to improve the properties of rubberized concrete to the extent that is comparable with the conventional concrete. This study highlighted the performance of the CFHS column under monotonic and cyclic loading using improved rubberized pozzolanic concrete with comparable properties to normal concrete.

2. Experimental programme

This study considered three types of columns subjected to monotonic and cyclic lateral loading. The specimens were square hollow steel column (SHS), normal concrete filled hollow steel column (NCFHS) and rubberized pozzolanic concrete filled hollow steel column (RuPCFHS). Two types of concrete infill were normal concrete (NC) and rubberized pozzolanic concrete (RuPC).

2.1. Characterization of the materials

Square hollow steel section with dimensions of 100×100 mm and 4 mm thickness was used in preparing the column specimens. Three coupon samples were taken from the flat surfaces of the hollow steel section and subjected to tensile testing to obtain the properties of the steel in accordance to BS EN 10002-1. The average measured properties of the steel were: yield stress, f_y = 264 N/mm^2, ultimate stress, f_u = 364 N/mm^2, and Young's Modulus, E_s = 223.8 kN/mm^2.

The concrete core of the NCFSH and RuPCFHS were prepared according to the mix proportion presented in Table 1. The concrete mixes were prepared using Class 1 ordinary Portland cement (OPC) with characteristic strength of 42.5 N/mm^2. The normal concrete (NC) was designed for 30 N/mm^2 at 28 days with a targeted slump value of 60 mm to 180 mm according to "Design of Normal Concrete Mixes" [14]. To produce the RuPC mix, crumb rubber from recycled tires with a size ranging from 0 mm to 2.4 mm was used to replace 5% of the total natural fine aggregate weight while fly ash obtained from a local coal-fired power plant was used to replace 10% by weight of cement. In order to achieve comparable strength with the NC, lower water-cement (w/c) ratio was used in RuPC. The RuPC mix was designed using the same method as in NC with the same design strength

(30 N/mm^2) and workability (60–180 mm slump), but with the usage of lower w/c ratio of 0.45, compared to 0.55 of NC. The crumb rubber and fly ash content was then calculated by the total weight of cement and fine aggregate content obtained from the mix design. The usage of lower w/c ratio reduced water among particles, thus reduced porosity in hardened concrete and consequently increasing the concrete strength [15]. Since the workability of RuPC mix was reduced due to the lower w/c ratio, 1.5% superplasticizer (SP) was used in the concrete mix to achieve the designed slump value.

Table 1. Mix proportion of concrete

Specimens	w/c	Cement (kg/m^3)	Fine aggregate (kg/m^3)	Coarse aggregate (kg/m^3)	Crumb rubber (kg/m^3)	Fly ash (kg/m^3)	Water (kg/m^3)	SP (%)
NC	0.55	425	1065	610	0	0	235	–
RuPC	0.45	468	917	615	48	52	235	1.5

The workability of the concrete was determined through the slump test upon completion of concrete mixing. The density of the concrete was calculated from the weight and volume of cubic specimens. Three cubic specimens ($100\times100\times100$ mm), three cylindrical specimens (Ø100 mm×H = 200 mm) and three prism specimens ($100 times 100\times500$ mm) were prepared and tested for compressive strength, splitting tensile strength and flexural strength, respectively, for each concrete mix. Table 2 presents the average results for the concrete properties. Both workabilities of NC and RuPC fall within the designed slump value. The usage of superplasticizer helped to improve the workability of RuPC in achieving the desired slump. Based on the results obtained, RuPC recorded comparable properties to that of NC. Both concrete recorded nearly similar densities. The hardened properties of RuPC were slightly higher than NC with 4.9%, 3.1% and 8.2% increment in compressive, splitting tensile and flexural strength, respectively.

Table 2. Properties of concrete at 28 days

Specimen	Slump (mm)	Density (kg/m^3)	Compressive strength (N/mm^2)	Splitting tensile strength (N/mm^2)	Flexural strength (N/mm^2)
NC	88	2293	34.8	3.2	4.9
RuPC	74	2292	36.5	3.3	5.3

2.2. Characterization of the specimens

In order to study the behaviour of the SHS, NCFHS and RuPCFHS subjected to monotonic and cyclic lateral loads, hot-rolled hollow sections were used and filled with two distinct concrete mixes: normal concrete (NC) and rubberized pozzolanic concrete

(RuPC). RuPC was obtained by replacing 5% of the total fine aggregate weight with crumb rubber. A total of twelve column specimens with a height of 1000 mm were prepared. The columns were comprised of four square hollow steel columns (SHS), four normal concrete filled hollow steel columns (NCFHS) and four rubberized pozzolanic concrete filled hollow steel columns (RuPCFHS) for testing under monotonic and cyclic lateral loadings as shown in Table 3. SHS, NCFHS and RuPCFHS tested without axial load were labelled as SHS-0, NCFHS-0 and RuPCFHS-0, respectively, while columns tested with the inclusion of axial load was labelled as SHS-20, NCFHS-20 and RuPCFHS-20, respectively. The columns were welded onto base plates that were later installed to the testing setup. The schematic diagram of the column specimens is presented in Fig. 1. Fresh concrete was poured into the hollow steel section, vibrated and left curing for 28 days before being tested.

Table 3. Column specimens for monotonic and cyclic testing

Column specimens	Infill	Monotonic		Cyclic	
		0% axial	20% axial	0% axial	20% axial
SHS	–	1	1	1	1
NCFHS	NC	1	1	1	1
RuPCFHS	RuPC	1	1	1	1

(a) Side view of column   (b) Plan view of column
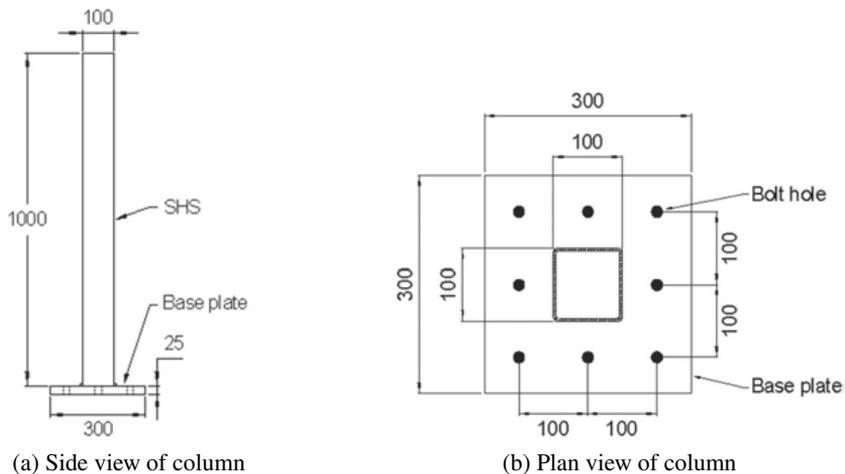
Fig. 1. Schematic drawing of column specimens

2.3. Testing setup

Three types of column specimens: square hollow steel column (SHS), normal concrete filled hollow steel column (NCFHS) and rubberized pozzolanic concrete filled hollow steel column (RuPCFHS) were tested. The adopted setup for investigating the behaviour of the

column specimens subjected to monotonic and cyclic lateral load are presented in Fig. 2
and Fig. 3, respectively. The bottom section of the column is fixed while the lateral load
and axial load were applied at the top section. Two sets of testing setup for monotonic
and cyclic tests were exposed to the column including axial load. Two types of axial load
conditions were applied during the lateral loading tests which were without axial load
(0% axial) and with axial load (20% axial load), calculated from the axial capacity of the
column specimens. The axial load was applied to the columns through the secured hinge
system which allowed the movement of the column in one direction while maintaining the
axial load applied to the column throughout the testing. The lateral force was applied at
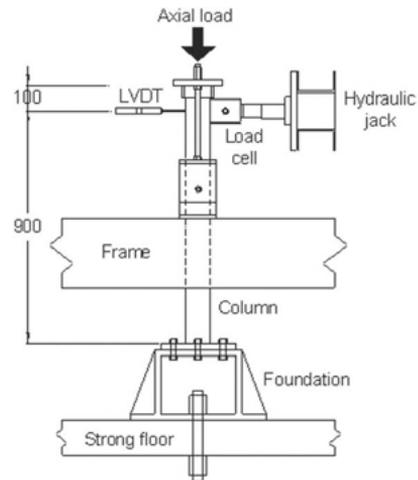

(a) Test setup without axial load

(b) Test setup with axial load
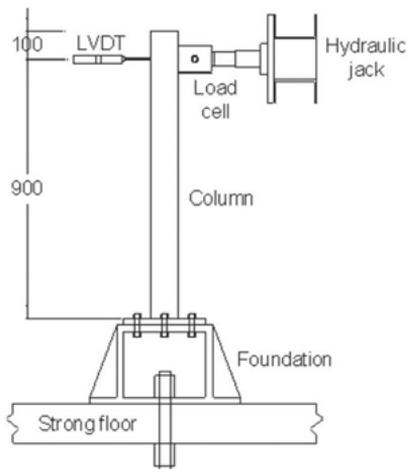
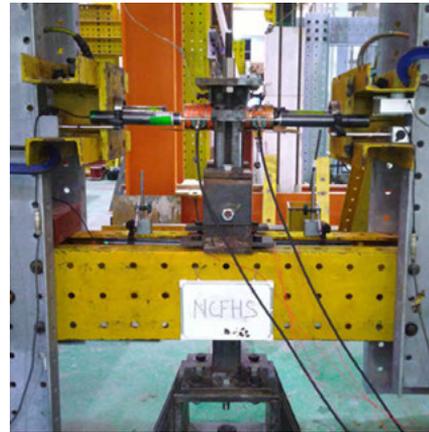(c) Schematic drawing of test setup without
axial load

(d) Schematic drawing of test setup with
axial load

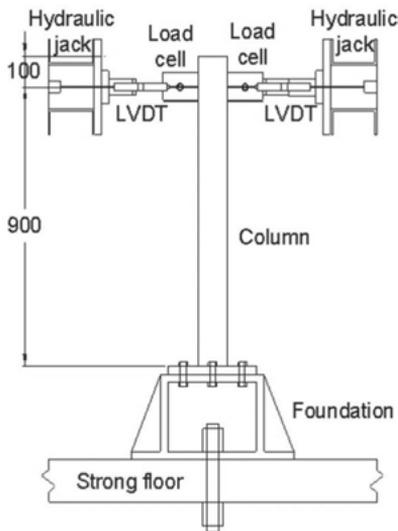Fig. 2. Column testing under monotonic lateral load

the top side of the column using hydraulic jack. In monotonic testing, the columns were pushed until maximum lateral capacity was achieved. The cyclic load test was carried out under deformation-control testing in compliance to FEMA 461 [16] consisting of 10 repeated cycles of increasing deformation amplitudes. The targeted maximum deformation was estimated from the results obtained through monotonic testing. Figure 4 show the deformation-controlled loading history as suggested in FEMA 461.
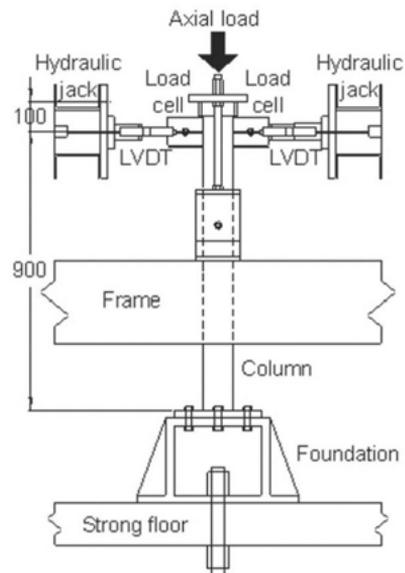
(a) Test setup without axial load   (b) Test setup with axial load

(c) Schematic diagram of test setup without   (d) Schematic diagram of test setup with
             axial load   axial load

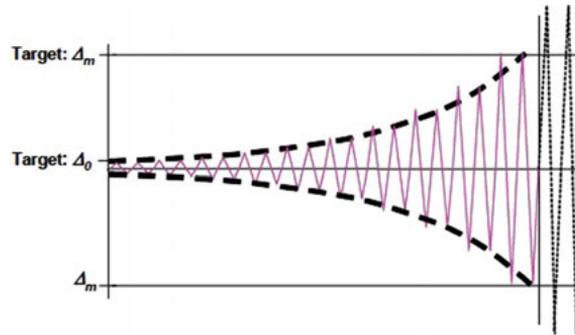Fig. 3. Column testing under cyclic lateral load

Fig. 4. FEMA 461 cyclic loading history [16]

3. Results and discussion

3.1. Monotonic testing of columns

The capacity curves obtained from laboratory testing subjected to monotonic loading for all column samples and testing conditions are shown in Fig. 5. For testing of columns under lateral load without axial loads, SHS-0 exhibits the lowest capacity at lower displacement, followed by RuPCFHS-0 and NCFHS-0 with an increment of 32% and 36%, respectively. The difference in the strength of NCFHS-0 and RuPCFHS-0 was about 4%, with a similar trend of the curve for both columns. The concrete infill is shown to give a significant contribution to the increase in lateral capacity and the displacement capability of CFHS, regardless of the type of concrete used. However, RuPCFHS-0 reached its capacity at lower displacement compared to NCFHS-0 with 17% difference due to the lower lateral capacity of RuPCFHS-0. In terms of elasticity, SHS show higher elasticity with lower gradient
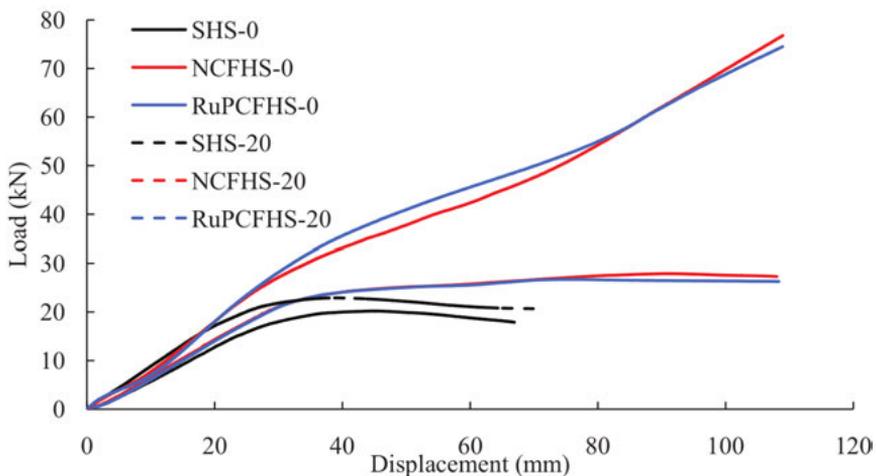

Fig. 5. Load-deflection curves of columns under lateral load

observed in the elastic region of the curve compared to CFHS. The maximum lateral capacity and the displacement at maximum capacity of the tested columns are shown in Table 4.

Table 4. Column specimens for monotonic and cyclic testing

Sample	Axial load (%)	Maximum load (kN)	Deflection at max. load (mm)
SHS	0	20.2	43.3
	20	23.0	39.5
NCFHS	0	27.5	91.1
	20	–	–
RuPCFHS	0	26.6	75.6
	20	–	–

The application of 20% axial load onto the column specimens shows a similar trend of lateral capacity among the column specimens in which SHS exhibit the lowest capacity followed by the CFHS. When the axial load was applied to the column, the capacity and the displacement of the columns were increased. When 20% axial load was applied, the maximum lateral capacity of SHS increased by about 13%. However, SHS-20 failed at lower displacement compared to SHS-0. Although the application of axial load increased the capacity of SHS, it was still lower than NCFHS-0 and RuPCFHS-0, highlighting the significant contribution of concrete infill in the overall performance of CFHS regardless of the axial load condition. The same result was observed for NCFHS-20 and RuPCFHS-20 where the lateral capacity was increased significantly when 20% axial load was applied to the column. NCFHS-20 and RuPCFHS-20 behaved in a similar pattern in the early elastic phase. However, RuPCFHS-20 exhibited higher lateral capacity at the displacement of 20 mm to 80 mm. At 60 mm deflection, RuPCFHS-20 recorded 7.8% higher lateral capacity compared to NCFHS-20. However, the maximum capacity of the NCFHS-20 and RuPCFHS-20 was undetermined due to the limitation of the testing setup in which the capacity of the testing setup was reached.

3.2. Cyclic testing of columns

Hysteresis curves are the most important outcome of quasi-static cyclic loading in the calculation of initial stiffness of the deformation of specimens, degradation in the stiffness and strength at each cyclic load and energy dissipation of specimens. In order to obtain hysteresis loops, the applied force at each cycle of loading is plotted against the measured displacement. The backbone curve later can be obtained by connecting the envelopes of force-displacement points of each cycle. From backbone curves, the initial stiffness of the specimen and the change in the lateral stiffness and strength can be calculated.

Figure 6 presents the hysteresis curve and backbone curve whereas Table 5 presents the initial stiffness and reduced stiffness of square hollow steel column (SHS) after being subjected to lateral cyclic loadings. Based on the results, SHS (0% axial) showed higher stiffness (0.69 kN/mm) at the beginning of the test compared to the stiffness at nine cycles of the loadings. The lateral stiffness of the specimen is reduced to 0.55 kN/mm before reaching its ultimate load. The reduction in stiffness was due to the development of local deformation that was developed at the bottom part of the column. When 20% axial was applied, SHS
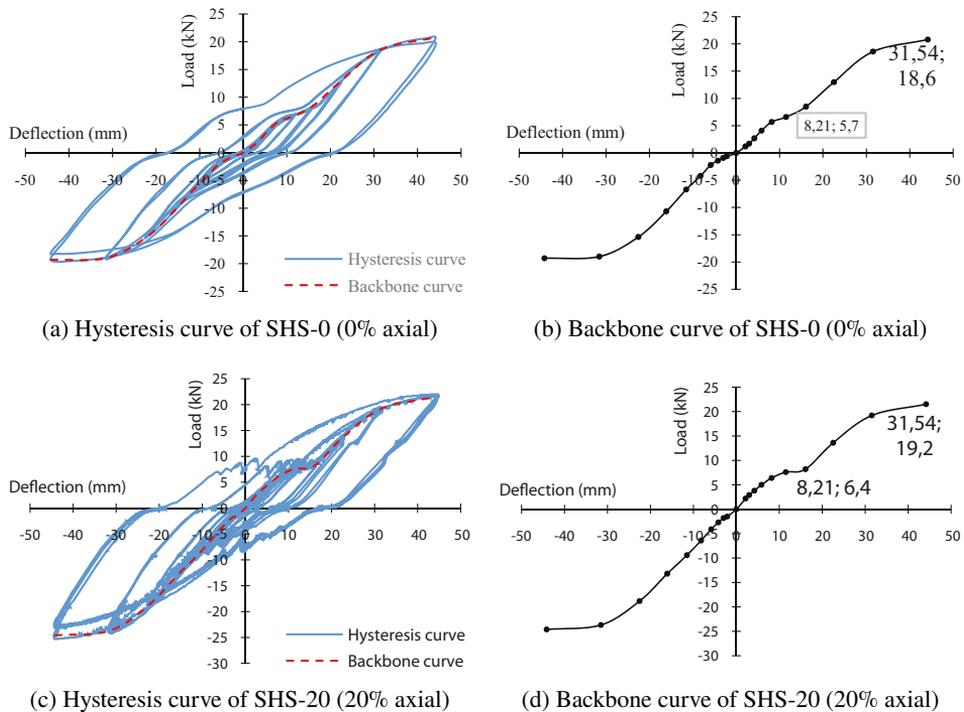

(a) Hysteresis curve of SHS-0 (0% axial)

(b) Backbone curve of SHS-0 (0% axial)

(c) Hysteresis curve of SHS-20 (20% axial)

(d) Backbone curve of SHS-20 (20% axial)

Fig. 6. Hysteresis and backbone curve of SHS

Table 5. Initial and second stiffness of SHS

Sample	SHS (0% axial)	SHS (20% axial)
Lateral load (P_1)	5.7 kN	6.4 kN
Deflection (d_1)	8.21 mm	8.21 mm
Initial stiffness (k_1)	0.69 kN/mm	0.78 kN/mm
Lateral load (P_2)	18.6 kN	19.2 kN
Deflection (d_2)	31.54 mm	31.54 mm
Reduced stiffness	0.55 kN/mm	0.55 kN/mm

displayed higher initial stiffness of 0.78 kN/mm. After a few cycles of loading, the lateral
stiffness reduced to 0.55 kN/mm, indicating a 29.5% reduction in the initial stiffness of the
specimen. Compared to SHS without axial load, the application of 20% axial load on the
column specimen increases the initial stiffness by 11.5%. However, the reduced stiffness
of SHS with and without axial load column after a few cycles of loading was the same,
indicating the same behaviour of columns after the formation of local failure.

Figure 7 and Table 6 display the obtained hysteresis, backbone curve and calculated stiff-
ness, respectively, for normal concrete filled hollow steel column (NCFHS). The NCFHS
exhibited higher initial stiffness (0.79 kN/mm) compared to SHS without axial load, with
a 14.5% increment in the lateral stiffness. The increase in stiffness is contributed by the
infill concrete in the NCFHS specimen which improves the overall strength of the column.
The backbone curve shows the stiffness of the column reduced to 0.65 kN/mm which is
more than that of SHS with and without axial load. Higher initial stiffness (0.82 kN/mm)
was obtained for the NCFHS with 20% axial load. The application of 20% axial load on
the column specimen increases the initial stiffness by 8.9%. When loading was applied for
further cycles, the stiffness of the column specimens reduced to 0.64 kN/mm, indicating a
22% reduction in stiffness. The reduction in stiffness occurred after the lateral load exceeds
about 30 kN. When the cyclic load was further applied, the concrete infill in the column
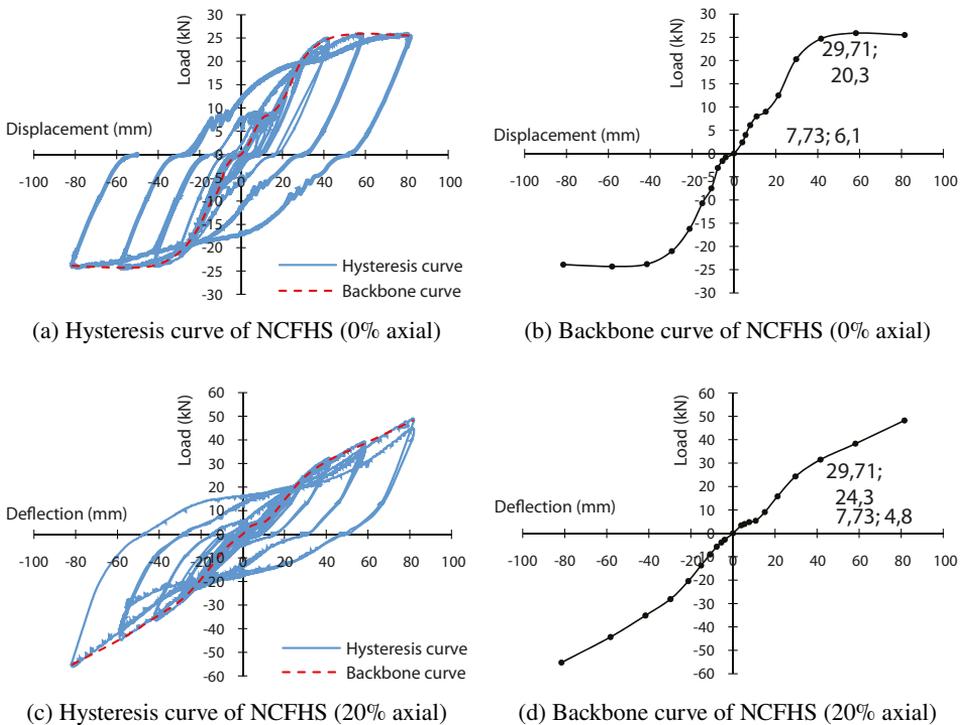specimen developed cracks, thus reducing the stiffness of the column.

(a) Hysteresis curve of NCFHS (0% axial)   (b) Backbone curve of NCFHS (0% axial)

(c) Hysteresis curve of NCFHS (20% axial)   (d) Backbone curve of NCFHS (20% axial)

Fig. 7. Hysteresis and backbone curve of NCFHS

Table 6. Initial and second stiffness of NCFHS

Sample	NCFHS (0% axial)	NCFHS (20% axial)
Lateral load (P_1)	6.1 kN	4.8 kN
Deflection (d_1)	7.73 mm	7.73 mm
Initial stiffness (k_1)	0.79 kN/mm	0.62 kN/mm
Lateral load (P_2)	20.3 kN	24.3 kN
Deflection (d_2)	29.71 mm	29.71 mm
Reduced stiffness	0.65 kN/mm	0.89 kN/mm

The hysteresis and backbone curve for rubberized pozzolanic concrete filled hollow steel column (RuPCFHS) is presented in Fig. 8. As can be seen from Table 7, the specimen has an initial stiffness of 0.74 kN/mm. The initial stiffness of the specimen is slightly lower when compared to the NCFHS with a 6% difference. The backbone curve shows the stiffness of the column reduced to 0.58 kN/mm which lay in between the NCFHS and the SHS. Similar behaviour for other column specimens, when the axial load was applied to the column specimen, higher initial stiffness (0.91 kN/mm) was recorded for the RuPCFHS

(a) Hysteresis curve of RuPCHS (0% axial)

(b) Backbone curve of RuPCHS (0% axial)

(c) Hysteresis curve of RuPCHS (20% axial)

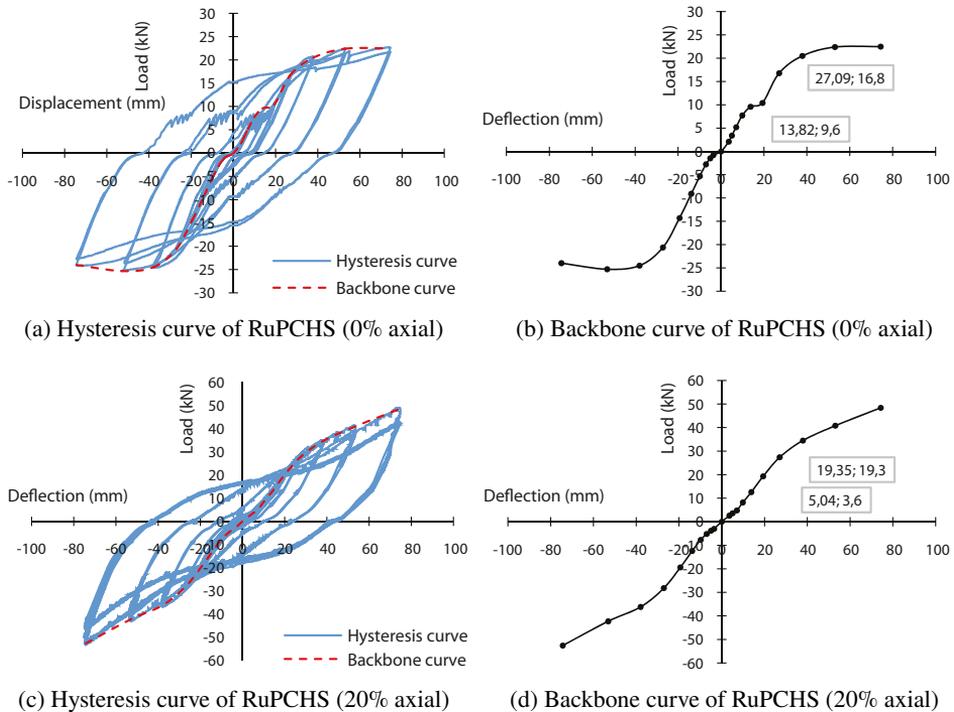(d) Backbone curve of RuPCHS (20% axial)

Fig. 8. Hysteresis and backbone curve of RuPCFHS

and the highest compared to other column specimens. The application of 20% axial load on the column specimen increased the initial stiffness by 23% compared to without axial load. When cyclic loading was applied for further cycles, the stiffness of the column specimens reduced to 0.71 kN/mm, indicating a 22% reduction in stiffness, the same value recorded by NCFHS with axial load. When lateral load exceeded 30 kN, the stiffness of the specimens was reduced as shown in the backbone curve where the gradient of the curve becomes sloppier. Further application of cyclic load resulted in the failure of the concrete infilled, reducing the latter stiffness of the column.

Table 7. Initial and second stiffness of RuPCFHS

Sample	RuPCFHS (0% axial)	RuPCFHS (20% axial)
Lateral load (P_1)	9.6 kN	3.6 kN
Deflection (d_1)	13.82 mm	5.04 mm
Initial stiffness (k_1)	0.69 kN/mm	0.71 kN/mm
Lateral load (P_2)	16.8 kN	19.3 kN
Deflection (d_2)	27.09 mm	19.35 mm
Reduced stiffness	0.52 kN/mm	1.10 kN/mm

Table 8 presents the summarized result of the stiffness of all columns specimens tested under cyclic load. For column specimens without axial load, the SHS recorded the lowest initial and reduced stiffness followed by the RuPCFHS and the NCFHS. The NCFHS shows the lowest reduction in stiffness (17.7%) whereas the RuPCFHS has the highest reduction in stiffness (21.6%). When 20% axial load was applied on the columns, the stiffness of the HS reduced about 29.5% after a few cycles of lateral load which was the highest reduction

Table 8. Initial and second stiffness for all column specimens

0% axial			
Column	k_1 (kN/mm)	k (kN/mm)	Difference (%)
SHS	0.69	0.55	−20.3
NCFHS	0.79	0.65	−17.7
RuPCFHS	0.69	0.52	−24.6
20% axial			
Column	k_1 (kN/mm)	k (kN/mm)	Difference (%)
SHS	0.78	0.65	-16.7
NCFHS	0.62	0.89	+30.3
RuPCFHS	0.71	1.10	+54.9

among column specimens with applied axial load. Although the RuPCFHS recorded the highest initial and later stiffness, the difference between the two stiffness was similar for the RuPCFHS and the NCFHS with a 22% reduction. Based on the results, the stiffness of the specimens reduced after being subjected to lateral cyclic load. After a few cycles of cyclic load applied, the stiffness of each column tends to decrease before reaching the maximum capacity. The reduction in stiffness of the specimens is caused by the occurrence of local deformation at the bottom part of the column. For the CFHS, the concrete infill began to fail after several cycles of loading and reduced the load-bearing capacity of the column.

The energy dissipation capacity of the studied columns was calculated using the obtained backbone curves by calculating the area below the curves. Table 9 presents the energy dissipation of all column specimens. For columns tested without axial load, SHS showed the lowest energy dissipation capability. When concrete infill was introduced, the energy dissipation increased significantly. NCFHS exhibited higher energy dissipation compared to RuPCFHS for about 21%. The same trend was observed in the results obtained from cyclic load testing of the column with axial load. Higher energy dissipation capability was observed on NCFHS, followed by RuPCFHS and HS. When 20% axial load was applied to the column, the energy dissipation of column specimens is increased. SHS specimens recorded the lowest improvement in energy dissipation capability with only 4.8%. Despite the highest energy dissipation capability of NCFHS when compared to other specimens, the increment in energy dissipation for NCFHS is 42.3% when 20% axial load was applied on the column during the cyclic testing. The difference between both NCFHS and RuPCFHS was reduced to only 1.6% compared to specimens without axial load. A significant increase in energy dissipation was observed for RuPCFHS when the axial load was applied to the column specimen. The increase in energy dissipation capability for RuPCFHS is 78.3%.

Table 9. Energy dissipation of the column specimens

| Column	Energy dissipation (kNmm)		Difference (%)
	0% axial	20% axial	
SHS	537.4	563.4	4.8
NCFHS	1571.0	2234.9	42.3
RuPCFHS	1233.7	2199.9	78.3

3.3. Failure mechanism of columns

The failure mechanism of the column was presented in terms of the location of visible deformation developed at the column surface. The location of the failure was measured from the top surface of the base plate to the tip of the deformation. Figure 9 presents the deformation developed for all tested columns. Based on the figures, the failure deformation was developed at the bottom section of all columns. Concave deformation of steel was observed for SHS for both axial load conditions. The location of deformation recorded

for SHS without axial load was 45 mm measured from the base plate, and 40 mm for specimens with axial load. The deformation recorded for NCFHS without and with axial load was 65 mm and 60 mm, respectively. Convex deformation was observed at the failure point. The convex-shaped deformation of NCFHS was contributed by the failure of the concrete infill. When the lateral load was applied to the specimens, the infill concrete tends to crack at the location where the failure was observed. Then the broken concrete was forced to push the hollow steel outward when the load was continuously applied, forming the convex failure that can be seen at the surface of the hollow steel. The failure behaviour
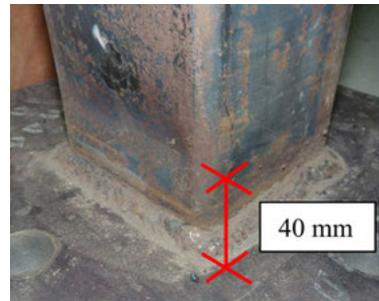
(a) Deformation of SHS-0   (b) Deformation of SHS-20
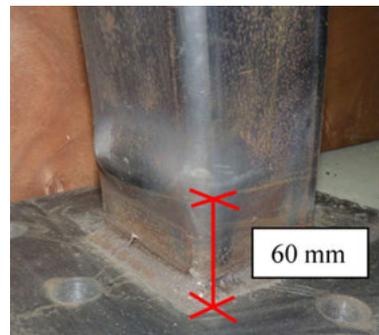
(c) Deformation of NCFHS-0   (d) Deformation of NCFHS-20

(e) Deformation of RuPCFHS-0   (f) Deformation of RuPCFHS-20

Fig. 9. Hysteresis and backbone curve of RuPCFHS

of RuPCFHS with and without axial load was identical to that of NCFHS. The deformation height recorded for RuPCFHS-0 and RuPCFHS-20 was 60 mm and 52 mm, respectively. The same behaviour of deformation was observed at the bottom part of the columns. The convex shaped deformation of RuPCFHS was due to the same reason as in NCFHS. SHS recorded the lowest failure height followed by RuPCFHS and NCFHS. Infilling SHS with concrete increased the stiffness of the column, causing the deformation to develop at a higher point. When the axial load was applied to the column during the testing, the failure was occurred at a lower height compared to the specimen without axial load.

The failure mechanism of the column subjected to cyclic loading was also observed and presented in Fig. 10, Fig. 11 and Fig. 12 for SHS, NCFHS and RuPCFHS, respectively. Generally, the failure of columns under cyclic loading had the same pattern as in monotonic testing where the failure occurred at the bottom part of the column. However, the failure occurred at two opposite faces of the column due to the application of cyclic loading. Concave deformation of steel was observed at a height of 45 mm for all SHS columns under both axial load conditions, which was the lowest height of deformation compared to NCFHS and RuPCFHS. When the concrete was filled in SHS, the deformation developed at a higher point. Convex deformation was observed for NCFHS-0 at 60 mm and 65 mm height, and 57 mm and 63 mm for NCFHS-20. The convex-shaped deformation was due to the same reason discussed in the failure mechanism of columns under monotonic loading. The failure behaviour of RuPCFHS with and without axial load was identical to that of

(a) Deformation of SHS-0 (left face)
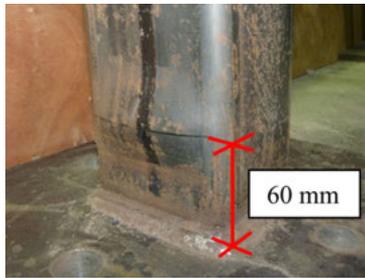

(b) Deformation of SHS-0 (right face)

(c) Deformation of SHS-20 (left face)

(d) Deformation of SHS-20 (right face)

Fig. 10. Deformation of SHS under cyclic loading

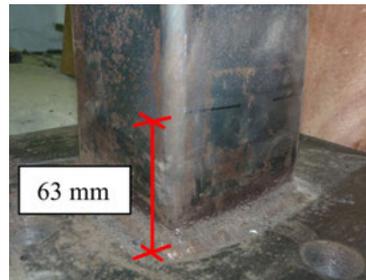536   MUHAMMAD NAJMI MOHAMAD ALI MASTOR et al.

(a) Deformation of NCFHS-0 (left face)

(b) Deformation of NCFHS-0 (right face)

(c) Deformation of NCFHS-20 (left face)

(d) Deformation of NCFHS-20 (right face)

Fig. 11. Deformation of NCFHS under cyclic loading

(a) Deformation of RuPCHS-0 (left face)

(b) Deformation of RuPCHS-0 (right face)

(c) Deformation of RuPCHS-20 (left face)

(d) Deformation of RuPCHS-20 (right face)

Fig. 12. Deformation of RuPCFHS under cyclic loading

NCFHS with convex-shaped deformation. The deformation observed for RuPCFHS-0 was 66 mm and 63 mm, while 55 mm and 70 mm for RuPCFHS-20. However, the pattern of the deformation location for NCFHS and RuPCFHS was inconsistent. This may be due to the different cracking behaviour of NC and RuPC when subjected to cyclic loading.

4. Conclusion

This study aims to determine the performance of concrete-filled hollow steel columns (CFHS) using modified rubberized pozzolanic concrete as infill materials in comparison to bare hollow steel columns and CFHS using normal concrete. Based on the experimental findings, it is concluded that infilling hollow steel columns significantly improve the lateral strength of the column, both in monotonic and cyclic regardless of the type of infill materials. The addition of concrete infill increases the overall strength and stiffness of the CFHS, resulting in a higher lateral capacity of the columns. SHS without infill showed the lowest monotonic and cyclic performance while both NCFHS and RuPCFHS behaved in quite a similar manner. When the axial load was applied on the column specimens, the lateral strength of all column specimens was increased where significant increment was observed for NCFHS and RuPCFHS where the application of axial load increases the confinement effect of the columns. Regarding the type of concrete infill, NCFHS and RuPCFHS behaved in quite a similar manner with a slight difference in performance under monotonic and cyclic loading. RuPCFHS exhibit slightly lower energy dissipation compared to NCFHS. However, RuPCFHS recorded the highest increment in the energy dissipation capability when 20% axial load was applied to the column when compared to the other columns. The modified rubberized pozzolanic concrete with equivalent strength to that of normal concrete have shown the possibility of the material to be used as an infill material for concrete filled hollow steel column.

Acknowledgements

References

[1] R. Abendeh, H.S. Ahmad, Y.M. Hunaiti, "Experimental studies on the behavior of concrete-filled steel tubes incorporating crumb rubber", *Journal of Constructional Steel Research*, 2016, vol. 122, pp. 251–260, DOI: 10.1016/j.jcsr.2016.03.022.

[2] G.D. Hatzigeorgiou, D.E. Beskos, "Minimum cost design of fibre-reinforced concrete-filled steel tubular columns", *Journal of Constructional Steel Research*, 2005, vol. 61, no. 2, pp. 167–182, DOI: 10.1016/j.jcsr.2004.06.003.

[3] P. Li, T. Zhang, C. Wang, "Behavior of Concrete-Filled Steel Tube Columns Subjected to Axial Compression", *Advances in Materials Science and Engineering*, 2018, vol. 2018, pp. 1–15, DOI: 10.1155/2018/4059675.

[4] A. Elremaily, A. Azizinamini, "Behavior and strength of circular concrete-filled tube columns", *Journal of Constructional Steel Research*, 2002, vol. 58, no. 12, pp. 1567–1591, DOI: 10.1016/S0143-974X(02)00005-6.

[5] L.H. Han, Y.F. Yang, Z. Tao, "Concrete-filled thin-walled steel SHS and RHS beam-columns subjected to cyclic loading", *Thin-Walled Structures*, 2003, vol. 41, no. 9, pp. 801–833, DOI: 10.1016/S0263-8231(03)00030-2.

[6] H. Yuan, J. Dang, T. Aoki, "Behavior of partially concrete- filled steel tube bridge piers under bi-directional seismic excitations", *Journal of Constructional Steel Research*, 2014, vol. 93, pp. 44–54, DOI: 10.1016/j.jcsr.2013.10.022.

[7] J. Xue, M. Shinozuka, "Rubberized concrete: A green structural material with enhanced energy-dissipation capability", *Construction and Building Materials*, 2013, vol. 42, pp. 196–204, DOI: 10.1016/j.conbuildmat.2013.01.005.

[8] M.Z. Siti Nurul Nureda, A.K. Mariyana, M. Iqbal Khiyon, M.S. Abdul Rahman, Z. Nurizaty, "Investigation on dynamic performance of concrete column crumb rubber steel and fiber concrete", *IOP Conference Series: Materials Science and Engineering*, 2017, vol. 271, no. 1, pp. 1–8, 10.1088/1757-899X/271/1/012082.

[9] A.P.C. Duarte, B.A. Silva, N. Silvestre, J. de Brito, E. Júlio, J.M. Castro, "Experimental study on short rubberized concrete-filled steel tubes under cyclic loading", *Composite Structures*, 2016, vol. 136, pp. 394–404, DOI: 10.1016/j.compstruct.2015.10.015.

[10] A. Silva, Y. Jiang, J.M. Castro, N. Silvestre, R. Monteiro, "Monotonic and cyclic flexural behaviour of square/rectangular rubberized concrete-filled steel tubes", *Journal of Constructional Steel Research*, 2017, vol. 139, pp. 385–396, DOI: 10.1016/j.jcsr.2017.09.006.

[11] M. Dong, M. Elchalakani, A. Karrech, M.F. Hassanein, T. Xie, B. Yang, "Behaviour and design of rubberised concrete filled steel tubes under combined loading conditions", *Thin-Walled Structures*, 2019, vol. 139, pp. 24–38, DOI: 10.1016/j.tws.2019.02.031.

[12] A.M. Najmi, A.K. Mariyana, P.N. Shek, Z. Nurizaty, "Hardened properties of concrete with different proportion of crumb rubber and fly ash", *IOP Conference Series: Materials Science and Engineering*, 2020, vol. 849, DOI: 10.1088/1757-899X/849/1/012038.

[13] A.M. Najmi, et al., "Effect of Water-Cement Ratio on Mechanical Properties of Rubberized Fly Ash Concrete", *IOP Conference Series: Materials Science and Engineering*, 2021, vol. 1144, DOI: 10.1088/1757-899X/1144/1/012017.

[14] D.C. Teychenné, R.E. Franklin, H.C. Erntroy, *Design of Normal Concrete Mixes*, Second Edition. United Kingdom: BUILDING RESEARCH ESTABLISHMENT, 1997.

[15] I.M. Nikbin, et al., "A comprehensive investigation into the effect of water to cement ratio and powder content on mechanical properties of self-compacting concrete", *Construction and Building Materials*, 2014, vol. 57, pp. 69–80, DOI: 10.1016/j.conbuildmat.2014.01.098.

[16] Applied Technology Council, *Interim Testing Protocols for Determining the Seismic Performance Characteristics of Structural and Nonstructural Components (FEMA 461)*, no. June. Redwood City: Federal Emergency Management Agency (FEMA), 2007, p. 138.